Interference Cancellation Characteristics of a BSCMA Adaptive Array Antenna in a DBF configuration

Toyohisa TANAKA, Ryu MIURA, and Yoshio KARASAWA
ATR Optical and Radio Communications Research Laboratories
2-2 Hikaridai, Seikacho, Sorakugun, Kyoto 619-02, Japan

1. Introduction

Subscribers to cellular phone systems, Personal Handy-phone System (PHS), and other mobile communication devices are rapidly increasing in number. In addition to this, communication services utilizing low orbiting satellites are scheduled to begin operations early in the 21st century. This calls into question the availability of frequency resources, or the lack of it.

In order to improve frequency utilization and prevent interference and multipath fading in wideband mobile communications, adaptive arrays are being vigorously researched. A digital beamforming antenna (DBF antenna) is one way of realizing an adaptive array. Rather than feed the output of each antenna element to analog devices such as a phase shifter or combiner, where synthesis and distribution occur, A/D converters are used. After conversion into digital data, digital signal processing takes place and multibeam formation, arrival direction estimation, interference elimination, and other such complex functions are achieved, making this an extremely versatile antenna. Needless to say, an immense amount of signal processing takes place and this leads to the assumption that a very large-scale circuit is needed. However, it is expected that rapid advances in device technology will lead to practicality.

ATR has developed a beam space CMA (constant modulus algorithm) adaptive array antenna (BSCMA adaptive array antenna) that may be suitable for mobile communications. It is comprised of an active array antenna and a digital signal processor [1-3]. This BSCMA adaptive array antenna has been applied to a trial system for testing in a large anechoic chamber. This paper presents the results of that experiment, which was carried out to capture and track characteristics of the desired wave including an interference wave. A $\pi/4$ shift QPSK signal with a data rate of 16 kbps was used.

2. BSCMA Adaptive Array Antenna System

A block diagram of the BSCMA adaptive array antenna system is shown in Fig. 1 and the system specifications are listed in Table 1. The antenna is a 16-element patch antenna arranged in a 4x4 square configuration with spacings of 1/2 the carrier frequency wavelength. Each element has its own LNA, BPF, down converter, LPF and A/D converter. All subsequent digital signal processing takes place on a single PC board that contains ten FPGAs (Field Programmable Gate Arrays). In each digital signal processing unit, a baseband signal passes through a quasi-coherent detector, Nyquist filtering takes place, and an FFT is spatially carried out to form a 16-beam orthogonal multibeam (see Fig. 2). Next, a maximum of four beams, all of which have a power level greater than a preset threshold, are selected and the phase offset of each beam inherent in the FFT is corrected. The CMA is then used to allow adaptive processing and the signal is finally sent to the demodulator.

3. Operating Principles of the BSCMA Adaptive Array

The CMA is a very effective algorithm for the constant envelope curve modulation method in that prior information is not needed; the so-called blind adaptive processing. First, an error value is obtained between a target convergence value σ and a value at the output of the CMA adaptive processor. Next, using the steepest descent method, an updated value is obtained for the weight value given to each input beam. When the n-th sample occurs and $W_m^{(n)}$ is taken as the weight vector and X_{mn} as the input of beam number m, the output value y_n is expressed as

$$y_n = \sum_{m=1}^{k} W_m^{(n)} \cdot X_{mn} \tag{1}$$

The weight at the $n+1$th sample is expressed as

$$W_m^{(n+1)}=W_m^{(n)}-\mu X^*_{mn} y_n(|y_n|^2-\sigma^2) \quad (2)$$

and is updated every sample. Here, X^*_{mn} is the conjugate prime number of the input beam vector, μ is the step constant, and σ is the target convergence value.

4. Experimental Setup

The layout of the experiment, which took place in a large anechoic chamber, is shown in Fig. 3. The transmitter and the antenna under test were on the same horizontal plane. Using the antenna as a reference point, the desired wave was radiated from an azimuth angle of 0° and the interference wave from an azimuth angle of -23° (left side). This angular difference corresponds to the antenna beam width and such an arrangement allows two signals to be concurrently entered onto one beam. The interference signal was a replica of the desired signal having a given delay. A 15-level PN code was used for the signal data. It was converted to a $\pi/4$-shifted QPSK signal and then divided and phase modulated by two vector signal generators (VSG) that were phase locked. The two waves were transmitted as coherent carrier waves at a frequency of 1.545 GHz from two circularly polarized patch antennas. After code conversion of the interference wave, it was digitally processed as a symbol delay signal; the symbol delay interval could be set to between 0 and 3.5 (maximum). The C/I ratio was adjusted by 3 dB, and this was based on the signal received (IF signal at each A/D converter input) by the wide beam antenna elements. The experiment was carried out under an environment of an approximately 53 dBHz C/No ratio for the desired wave of each element. Using the adaptive processor weight and selected beam number, experimental results were determined from the radiation pattern, which was calculated off-line. During the measurements, the BER of the demodulator data was also measured.

A planar view of the antenna pattern is shown in Fig. 2, where the angular change is expressed by the locus (dashed line). In order to determine the advantageous reception directions for the desired and interference waves, the azimuth angle was varied from -40° to +30°. Capture tracking characteristics were determined by measuring interference elimination characteristics, and this was done while keeping the differential angle constant between the two radiating sources, but varying the azimuth angle. As can be seen, the received wave pattern had a sliding image. The azimuth rotational speed was about 8°/sec; this is equivalent to traveling about 40 km/h on a curve with an 80 m radius.

5. Interference Cancellation Characteristics

The interference wave symbol delay and carrier wave relative phase were used as the measurement parameters. Throughout these measurements, the input beam was changed, but the weight value was not initialized. In order to vary the phase between the carriers of the desired and interference waves, a phase stretcher, which allowed the phase difference to be set at 0°(=φ ref), ±90 °, or 180°, was added to the output of the VSG. Measurements taken using interference symbol delays of 3.0, 1.0, and 0.25 as parameters and a roll angle of 0° are shown in Fig. 4(a), (b), (c), and (d), respectively. In each figure, the two locuses on the plot represent the directions of the desired and interference waves. The "antenna azimuth" gives an angle from the viewpoint of the antenna itself. The "scan azimuth" is the horizontal angle of the antenna during measurement, as shown in Fig. 3. For instance, if the "scan azimuth" is set to 0°, the desired wave is radiated from 0° of the "antenna azimuth", and the interference wave is radiated from 23°.

In Fig. 4(a) and (b), cases where the interference symbol delay was greater than 1.0, the results were excellent: stable capture tracking characteristics for the desired wave, interference suppression characteristics, and no bit errors during tracking. The average null depth for the interference wave was approximately less than -20dB during the measurement. Similar results were obtained for the various relative phase settings.

For Fig. 4(c) and (d), the symbol delay was the same (0.25), but the phase relation between the desired and interference waves was different. In the case of (c), both the desired and interference waves were accepted. On the other hand, in the case of (d), the delay wave acted as interference and suppression was carried out. This phenomenon was obviously due to the phase relation between the desired and interference waves at the antenna. Despite such results, no errors occurred during measurement.

Even though the BSCMA adaptive array antenna appears to have phase-dependent behavior when an interference wave has less than one symbol delay, the system functions to keep the output signal constant envelope curve, and this improves the BER characteristics in the long run.

6. Conclusion

Capturing and tracking characteristics were measured during interference suppression by a beam space CMA adaptive array antenna in a DBF configuration. Excellent interference elimination characteristics were obtained for symbol delays greater than 1. For symbol delay values of less than one, the system decided to adopt or reject the interference wave depending on the phase relation between the desired and interference waves, so as to realize better digital transmission quality.

Acknowledgment

The authors would like to thank Dr. Hideyuki Inomata, president of ATR Optical and Radio Communications Research Laboratories, for his constant guidance and encouragement.

References

[1] I. Chiba et al., IEICE Trans. (B-II), vol. J77-B-II, no. 3, pp. 130-138, Mar. 1994.

[2] T. Tanaka et al., IEICE Trans. (B-II), vol. J78-B-II, no. 9, pp. 602-610, Sep. 1995.

[3] T. Tanaka et al., IEICE Trans. Comm., vol. E78-B, no.11, pp. 1467-1473, Nov. 1995.

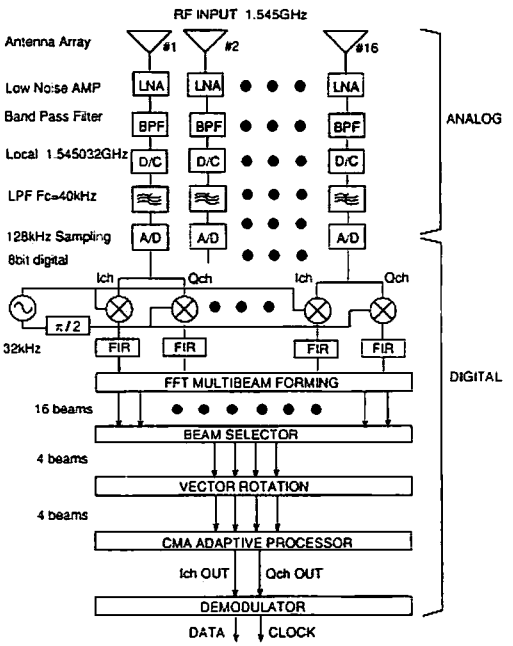

Fig. 1. BSCMA adaptive array antenna block diagram

Table 1. Experimental system specifications

Item	Specification
Number of antenna elements	16
RF frequency	1.545 GHz
IF frequency	32 kHz
A/D Sampling frequency	128 kHz
Bit accuracy of A/D	8 bit
Operational precision of multibeam formation	8 bit fixed point
Operational precision of adaptive processing	12 bit fixed point
Modulation scheme	π/4 shifted QPSK
Data rate	16 kbps
Transmittion data	15-level PN code

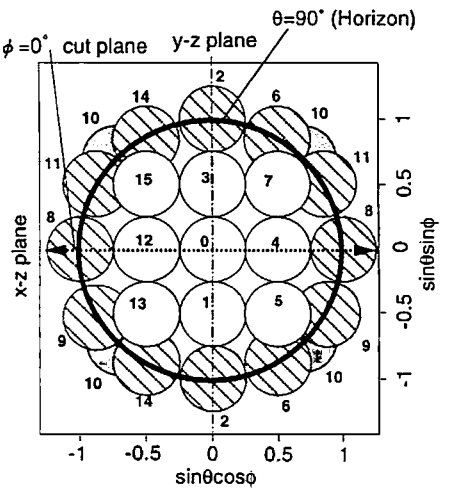

Fig. 2. Relation between beam number and directivity

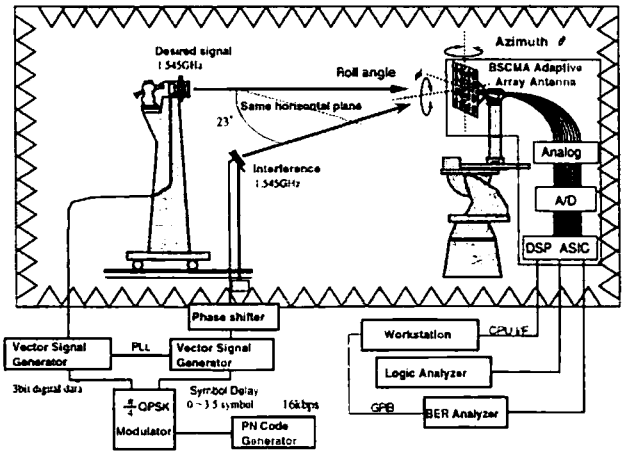

Fig. 3. Interference cancellation experimental setup

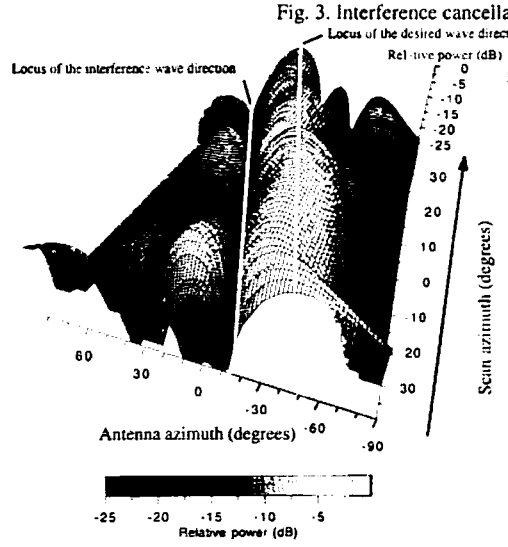

(a) Symbol delay 3.0

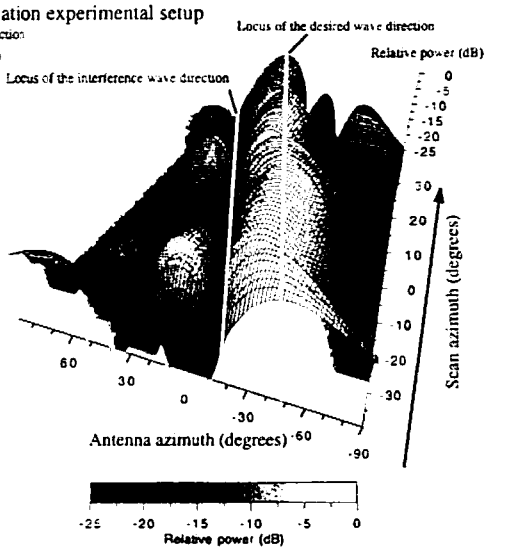

(b) Symbol delay 1.0

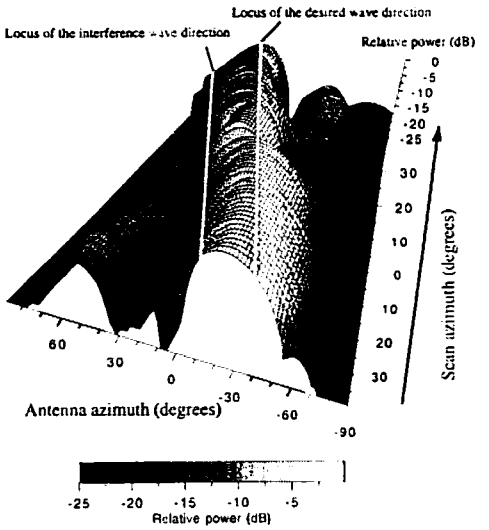

(c) Symbol delay 0.25, RF phase = φ ref

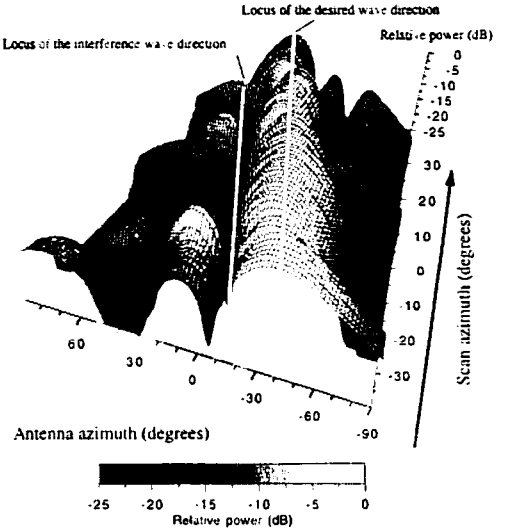

(d) Symbol delay 0.25, RF phase = φ ref +180°

Fig. 4. Capturing and tracking characteristics of the desired and interference waves